Fermi National Accelerator Laboratory

FERMILAB-Pub-95-091-A
April 1995

Decaying Λ cosmologies and statistical properties of gravitational lenses

L. F. Bloomfield Torres[◇] and I. Waga[*,◇]

[*] *NASA/Fermilab Astrophysics Center,*
Fermi National Accelerator Laboratory, Batavia, IL 60510

[◇] *Universidade Federal do Rio de Janeiro, Instituto de Física,*
Rio de Janeiro - RJ - Brasil -21943

Abstract

In this paper we investigate the statistical properties of gravitational lenses for models in which a cosmological term decreases with time as $\Lambda \propto a^{-m}$, where a is the scale factor and m is a parameter ($0 \leq m < 3$). We show that for given low values of the present matter density parameter Ω_{m0}, there is a wide range of values for m for which the lensing rate is significantly smaller than that in cosmological constant (Λ) models. We also show that models with low Ω_{m0} and $m \gtrsim 2$ have high likelihood to reproduce the observed lens statistics in the HST snapshot survey.

Key words: cosmology: theory - gravitational lensing.

1 Introduction

In the last five years or so, the statistics of gravitational lensing (Turner, Ostriker and Gott III 1984, hereafter TOG) has proven to be a powerful tool in constraining models of the universe, especially those with a cosmological constant (Λ). Cosmologies with a Λ-term have a long history and are now receiving considerable attention (see Carroll, Press and Turner 1992 for review). Spatially flat cosmological models with a cosmological constant have been suggested (Peebles 1984; Turner, Steigman & Krauss 1984) as a way to reconcile inflation with dynamical analyses on scales of $\sim 10h^{-1}$ Mpc, that indicate a value for the density parameter $\Omega_0 \sim 0.1$ to 0.3 (Peebles 1993). A cosmological constant also alters the transfer function for the density perturbations giving more power in the perturbation spectrum at large scales (as compared with standard CDM) in accordance with observations (Efstathiou *et al.* 1990; Lahav *et al.* 1991; Kofman *et al.* 1993). Besides, if the present value of the Hubble parameter is high, as indicated by some recent observations (Pierce *et. al.* 1994; Freedman *et. al.* 1994), a cosmological term will be the only way to get a theoretical age for a flat universe in accordance with current age estimates for globular clusters (Chaboyer 1994).

The idea that light could be focused by the gravitational lens effect was first suggested by Lodge (1919) near the beginning of the century. For several decades the subject of gravitational lensing had a quite slow development, but recently it started to become one of the most active research area in astrophysics and cosmology. There are several reasons for the current interest in gravitational lensing. On the cosmological side, after the works of Refsdal (1964) and Press & Gunn (1973), it was realized that cosmological parameters could be probed by the gravitational lensing effect. In the beginning it seemed that lensing properties were too insensitive and would only distinguish extreme cosmological models. Later on, Turner (1990) and Fukugita, Futamase & Kasai (1990) showed that a non-zero cosmological constant could significantly affect the statistics of gravitational lenses, especially in a low-density universe.

However, there are uncertainties in the study of the statistics of gravitational lensing (Mao 1991; Fukugita, Futamase, Kasai & Turner 1992, hereafter FFKT). For example, the lens effect depends considerably on how the mass is distributed in the lensing galaxy. Hinshaw and Krauss (1987) showed that the introduction of a core in the isothermal sphere galaxy model (non-singular isothermal sphere) can significantly modify the statistical lensing properties. Another issue is what distance formula should be used: the angular diameter distance or the Dyer-Roeder distance? Related to this question is the kind of statistics to be applied (Ehlers & Schneider 1986; FFKT). We should also mention the important effect of magnification bias and other selection effects such as angular resolution, galaxy evolution and merging on lensing probabilities (TOG; Fukugita & Turner 1991, hereafter FT; Mao 1991; Mao & Kochaneck 1993; Rix, Maoz, Turner & Fukugita 1994).

In spite of the uncertainties, the calculated rate of lensing in Λ-flat models, when confronted with the existing lensing observations, indicates that models with density parameter (Ω_{m0}) close to unity are most likely. For instance, Maoz & Rix (1993) claim that at present we should have $\Omega_\Lambda \lesssim 0.7$. So, it is becoming more and more difficult to make the dynamical estimates for Ω on scales $\sim 10h^{-1}$ Mpc compatible with a flat cosmological model with $\Lambda \neq 0$. It should be pointed out, however, that the lensing frequency of quasar images is considerably reduced if early-type galaxies ($z \gtrsim 0.5$) were dusty (Fukugita & Peebles (1994)).

The results above seem to favor open FRW models. There are however other possibilities. For example, Ratra and Quillen (1992) showed that, for a wide range of parameters, the predicted lensing rate is considerably reduced in a class of flat models (Peebles & Ratra 1988, Ratra & Peebles 1988) in which a scalar field plays the role of an effective cosmological "constant" that decreases with time. Some other models with a decreasing cosmological term were also proposed ((Ozer & Taha 1987a,b; Freese, Adams, Frieman & Mottola 1987; Chen & Wu 1990; Abdel-Rahman 1992; Carvalho, Lima & Waga 1992; Silveira & Waga 1994) and it would be interesting to know if they also predict a lower lensing rate. We can argue that we should expect a positive answer to this question. The reason is that usually in a varying Λ cosmological model, the distance to an object with redshift z is smaller than the distance to the same object in a constant Λ model with the same Ω_{m0}. So, the probability that light coming from the object is affected by a foreground galaxy is reduced in a decaying Λ cosmology. However this is only a qualitative argument, and it is clear that a quantitative treatment is necessary if we want to put limits on parameters of the models.

In this paper we address the above question to the special class of models proposed by Silveira and Waga (1994) in which a cosmological term decreases with time as $\Lambda \propto a^{-m}$, where a is the scale factor and $0 \leq m < 3$ is a constant. We show that these models also admit a large set of parameters for which the predicted lensing rate is much lower than that obtained in a constant Λ model with the same low value of Ω_{m0}. The paper is organized as follows: In section (2) the assumptions and basic equations of our models are presented. We exhibit expressions for two sorts of distance that we shall use, and discuss the corresponding statistics associated with them. In section (3) we model galaxies by the isothermal sphere density profile and obtain the predicted lensing probabilities and the distribution of image angular separation for some typical models previously chosen. In section (4) we compare the predictions of the models to observations and stress our main conclusions in section (5).

2 Decaying vacuum cosmological models – distance and optical depth formulas

Following Silveira and Waga we assume that the cosmic fluid is a non-interacting

mixture of non-relativistic matter and radiation. The cosmological term is assumed to be a time dependent quantity,

$$\Lambda = 3\tilde{\beta}a^{-m}, \tag{1}$$

where $\tilde{\beta} \geq 0$ is a constant and the factor 3 was inserted for mathematical convenience. We also assume that the vacuum decays only into relativistic particles such that matter is conserved ($\rho_m \propto a^{-3}$). As shown by Silveira and Waga (1994), the radiation energy density has two parts; one conserved ($\Omega_{r0}{H_0}^2(a_0/a)^4$) and a second one, ($\frac{3m\tilde{\beta}}{8\pi G(4-m)}a^{-m}$), that appears due to particle creation by the decaying vacuum. Here a_0 is the present value of the scale factor, $H_0 = 100\ h\ km\ s^{-1}\ Mpc^{-1}$ is the present value of the Hubble parameter ($h \simeq 0.5 - 1$) and $\Omega_{r0} = 4.3 \times 10^{-5}h^{-2}$ stands for the present value of the conserved radiation density parameter. In the following, subscripts 0 will always indicate present values.

The Einstein equations for the models we are considering reduce to

$$\left(\frac{\dot{a}}{a}\right)^2 = \Omega_{m0}H_0^2\left(\frac{a_0}{a}\right)^3 + \Omega_{x0}H_0^2\left(\frac{a_0}{a}\right)^m - \Omega_{k0}H_0^2\left(\frac{a_0}{a}\right)^2, \tag{2}$$

and

$$\frac{\ddot{a}}{a} = -\frac{1}{2}\Omega_{m0}H_0^2\left(\frac{a_0}{a}\right)^3 + \frac{(2-m)}{2}\Omega_{x0}H_0^2\left(\frac{a_0}{a}\right)^m, \tag{3}$$

where Ω_{m0} is the matter density parameter, $\Omega_{x0} = \frac{4\tilde{\beta}H_0^{-2}a_0^{-m}}{(4-m)}$ and $\Omega_{k0} = \frac{k}{H_0^2a_0^2}$.

Since we are mainly interested in the lensing properties of the models, only recent epochs have to be considered ($z \lesssim 5$). This justifies neglecting the conserved radiation energy density on the right hand side of (2) and (3). To have some grounds of comparison we have included the curvature term in (2) and will also consider the open FRW ($k = -1$) model.

The equations above are quite general and apply for a broad spectrum of models. Let us first consider the $k = 0$ case. For instance, if $m = 0$ the usual flat FRW model with a cosmological constant is recovered, whilst if $m = 2$ the above equations (with $\Omega_{k0} = 0$) are formally the same as those of the open FRW model. The same equations also appear in some string dominated cosmologies (Vilenkin 1984). Further, we would get the same equations if we had considered, besides matter , an exotic x-fluid with equation of state, $p_x = (\frac{m}{3} - 1)\rho_x$. Cosmologies having a fluid with this behavior were investigated by Fry (1985), Sahni, Feldman and Stebbins (1992), Feldman and Evrard (1993) and more recently by Martel (1995). We remark that all we shall discuss here also applies for these models. We should also mention that in the limit $\rho_m >> \rho_\phi$, the scalar field model analyzed by Ratra and Quillen has the same behavior as the one proposed here. This can be seen easily if we relate their parameter α with m as, $\alpha = \frac{2m}{3-m}$. It is clear however, that the models are different (unless $m = 0$) if $\Omega_{m0} \gtrsim \Omega_{x0}$ or during the x-component (vacuum) dominated era when, in fact, all the lensing properties we shall discuss are important.

In this paper we shall compare the following models:
Case A: $m = 0$, $\Omega_{m0} = 1$ and $k = 0$ (Einstein-de Sitter model).
Case B: $m = 2$, $\Omega_{m0} = 0.2$ and $k = 0$.
Case C: $m = 0$, $\Omega_{m0} = 0.2$ and $k = 0$ (Friedman-Lemaitre model).
Case D: $\Omega_{m0} = 0.2$, $\Omega_{z0} = 0$ and $k = -1$ (Open FRW model).
For the sake of completeness we have included case D in our analysis. It will be interesting to compare it with case B, which has similar field equations but has flat spatial sections. We also analyzed the case $m = 1$ and it turned out that it always has behavior between cases B and C, so we decided not to explicitly include it in our discussion.

For the flat models A, B and C, the angular diameter distance, $d_S(z_L, z_S)$, between two objects, one with redshift z_L and the other with z_S is given by,

$$d_S(z_L, z_S) = \frac{cH_0^{-1}}{1+z_S} \int_{z_L}^{z_S} \frac{dy}{\sqrt{\Omega_{m0}(1+y)^3 + (1-\Omega_{m0})(1+y)^m}}. \tag{4}$$

Equation (4) can be expressed in terms of the hypergeometric functions $F(a, b; c, z)$ as

$$\begin{aligned} d_S(z_L, z_S) \;=\; & \frac{2cH_0^{-1}}{(1+z_S)\sqrt{\Omega_{m0}}} \times \\ & \Big(\frac{1}{\sqrt{1+z_L}} F\Big(\frac{1}{2}, \frac{1}{6-2m}; \frac{7-2m}{6-2m}, -\frac{1-\Omega_{mo}}{\Omega_{m0}}(1+z_L)^{m-3}\Big) - \\ & \frac{1}{\sqrt{1+z_S}} F\Big(\frac{1}{2}, \frac{1}{6-2m}; \frac{7-2m}{6-2m}, -\frac{1-\Omega_{mo}}{\Omega_{m0}}(1+z_S)^{m-3}\Big)\Big). \end{aligned} \tag{5}$$

For some special values of m, the hypergeometric function in (5) can be reduced to elementary functions. This can be done, for instance, for $m = 2$ if we use the relation, $F(1/2, 1/2; 3/2, -x^2) = x^{-1} \sinh^{-1}(x)$. For the Einstein-de Sitter model equation (4) can easily be integrated giving

$$d_S(z_L, z_S) = \frac{2cH_0^{-1}}{1+z_S} \left[(1+z_L)^{-1/2} - (1+z_S)^{-1/2}\right]. \tag{6}$$

In fact, we can obtain (6) from (5), by observing that in the limit $\Omega_{m0} \to 1$ the hypergeometric function also goes to unity.

In the case of open models, the angular diameter distance can be expressed as (FFKT)

$$\begin{aligned} d_S(z_L, z_S) \;=\; & \frac{2cH_0^{-1}}{\Omega_{m0}^2(1+z_L)(1+z_S)^2} \{(2 - \Omega_{m0} + \Omega_{m0} z_S) \times \\ & \sqrt{1+\Omega_{m0} z_L} - (2 - \Omega_{m0} + \Omega_{m0} z_L)\sqrt{1+\Omega_{m0} z_S}\}. \end{aligned} \tag{7}$$

The differential probability, $d\tau$, that a line of sight intersects a galaxy at redshift z_L in the interval dz_L from a population with number density n_l is (TOG; Peebles 1993)

$$d\tau = -n_l \sigma c \frac{dt}{dz_L} dz_L, \tag{8}$$

where from (2) we have

$$\frac{dt}{dz} = -\frac{H^{-1}(z)}{1+z} = -\frac{H_0^{-1}}{1+z}\left(\Omega_{m0}(1+z)^3 + \Omega_{x0}(1+z)^m - \Omega_{k0}(1+z)^2\right)^{-1/2}. \tag{9}$$

The cross section (σ) in (8) is given by

$$\sigma = \pi a_{cr}^2, \tag{10}$$

where a_{cr} is the effective radius of the lens, that is, a_{cr} is the maximum distance of the lens from the optical axes for which multiple image is possible.

The total optical depth (τ) is obtained by integrating $d\tau$ along the line of sight from 0 to z_S, that is

$$\tau = \int_0^{z_S} d\tau = -\int_0^{z_S} n_l \sigma c \frac{dt}{dz_L} dz_L. \tag{11}$$

In the angular diameter distance definition it is assumed that the matter in the universe is homogeneously distributed. However the gravitational lens effect will not occur in a smooth universe. Only if matter is clumped, as in the real universe, can this effect take place. A distance formula that takes matter clumping into account was proposed by Dyer and Roeder (1972, 1973) and is known as the Dyer-Roeder (DR) distance. Here we will consider two extreme cases. We have already discussed the first one in which the smoothness parameter ($\tilde{\alpha}$), where $0 \leq \tilde{\alpha} \leq 1$, is equal to one (filled beam DR distance or angular diameter distance). The other extreme case, $\tilde{\alpha} = 0$, is called the DR empty beam distance (Schneider, Ehlers and Falco 1992).

For the models under consideration, the empty beam DR distance is given by (FFKT)

$$d_{DR}(z_L, z_S) = cH_0^{-1}(1+z_L) \times \int_{z_L}^{z_S} \frac{(1+y)^{-2} dy}{\sqrt{\Omega_{m0}(1+y)^3 + (1-\Omega_{m0}-\Omega_{x0})(1+y)^2 + \Omega_{x0}(1+y)^m}} \tag{12}$$

Notice that for the same Ω_{m0}, flat models ($\Omega_{m0} + \Omega_{x0} = 1$) with $m = 2$ and open models ($\Omega_{x0} = 0$) have the same empty beam distance. For the open (just make $m = 2$ in (13)) and flat models, equation (12) can be expressed in terms of hypergeometric functions as

$$d_{DR}(z_L, z_S) = \frac{2cH_0^{-1}(1+z_L)}{5\sqrt{\Omega_{m0}}} \times$$
$$((1+z_L)^{-5/2} F(\frac{1}{2}, \frac{5}{6-2m}; \frac{11-2m}{6-2m}, -\frac{1-\Omega_{mo}}{\Omega_{m0}}(1+z_L)^{m-3}) -$$
$$(1+z_S)^{-5/2} F(\frac{1}{2}, \frac{5}{6-2m}; \frac{11-2m}{6-2m}, -\frac{1-\Omega_{mo}}{\Omega_{m0}}(1+z_S)^{m-3})). \quad (13)$$

Again, in the limit $\Omega_{m0} \rightarrow 1$ the hypergeometric function goes to unity and (13) simplifies to

$$d_{DR}(z_L, z_S) = \frac{2cH_0^{-1}(1+z_L)}{5\sqrt{\Omega_{m0}}}((1+z_L)^{-5/2} - (1+z_S)^{-5/2}). \quad (14)$$

In obtaining the probability of multiple images in (11), we considered a random line of sight to the source at z_S, calculated the expected number of lenses ($d\tau$) in the redshift interval dz_L around z_L, and then integrated $d\tau$ from 0 to z_S. Ehlers and Schneider (1986) observed that in a self-consistent treatment of probabilities in a clumpy universe, the random variable should be the position of the source on a sphere at z_S (and not the line of sight to the source). They then proposed a new derivation for the optical depth that is called the ES probability. The Ehlers-Schneider differential probability ($d\tau_{ES}$) can be expressed as (FFKT)

$$d\tau_{ES} = \left(\frac{d_{DR}(0, z_S)}{d_S(0, z_S)}\right)^2 \left(\frac{d_S(0, z_L)}{d_{DR}(0, z_L)}\right)^2 d\tau, \quad (15)$$

where in $d\tau$ (given by equation (8)), the empty beam distance should be used. By integrating (15) from 0 to z_S we obtain the total ES optical depth.

In Figures 1*a* and 1*b* we present the quantity D_{OS}/cH_0^{-1} for the filled and empty beam distances. We also show in Figures 2*a* and 2*b* , also for both distances, the combination $D_{OL}D_{LS}/(D_{OS}cH_0^{-1})$ that appears, through a_{cr}, in the differential probability formulas. We are following the TOG and FFKT notation, such that $D_{LS} = d(z_L, z_S)$, $D_{OS} = d(0, z_S)$ and $D_{OL} = d(0, z_L)$.

3 The isothermal sphere galaxy model

Let us now consider the isothermal sphere model for galaxies. This model is characterized by two parameters, namely, the core radius (r_c) and the one-component velocity dispersion ($\sigma_{||}$). Following Hinshaw and Krauss (1987), we assume the lens galaxy to have the following density profile

$$\rho(r) = \frac{\sigma_{||}^2}{2\pi G(r^2 + {r_c}^2)}. \quad (16)$$

The surface mass density of the lens on the lens plane is given by (Bourassa & Kantowski 1975)

$$\Sigma(a) = 2\int_a^\infty \rho(r)\frac{rdr}{\sqrt{r^2-a^2}} = \frac{\sigma_{||}^2}{2G\sqrt{a^2+r_c^2}}, \tag{17}$$

and the projected mass interior to the impact parameter b is,

$$M(b) = 2\pi\int_0^b a\Sigma(a)da = \frac{\pi\sigma_{||}^2}{G}\left[\sqrt{b^2+r_c^2}-r_c\right]. \tag{18}$$

The bending angle is

$$\alpha = \frac{4GM(b)}{c^2 b} = \alpha_0\frac{\sqrt{b^2+r_c^2}-r_c}{b}, \tag{19}$$

where $\alpha_0 = 4\pi\left(\frac{\sigma_{||}}{c}\right)^2 \approx 1.8''(\sigma_{||}/250\ kms^{-1})^2$ denotes the constant bending angle for the singular isothermal sphere case (SIS), obtained by taking the limit $r_c \to 0$.

By using simple geometry it is easy to see from Figure 3 that

$$l + b = \frac{D_{OL}D_{LS}}{D_{OS}}\alpha, \tag{20}$$

where l is the distance from the lensing galaxy to the unperturbed line of sight. It follows from (19) and (20) that, if $r_c = 0$ (SIS case), the maximum value of l for multiple images (a_{cr}) is given by

$$a_{cr}(0) = \frac{D_{OL}D_{LS}}{D_{OS}}\alpha_0. \tag{21}$$

If $r_c \neq 0$ (NSIS), by substituting (19) in (20) we get the cubic equation,

$$b^3 + 2lb^2 + (l^2 + 2r_c a_{cr}(0) - a_{cr}^2(0))b + 2lr_c a_{cr}(0) = 0. \tag{22}$$

The number of real and distinct solutions of (22) depends on the sign of its discriminant. Hinshaw and Krauss (1987) showed that in order to produce multiple images, the lens maximum distance from the unperturbed line of sight should have the following expression

$$a_{cr} = a_{cr}(0)\left[(1+5\beta-\frac{1}{2}\beta^2) - \frac{1}{2}\beta^{1/2}(\beta+4)^{3/2}\right]^{\frac{1}{2}}, \tag{23}$$

where $\beta = r_c/a_{cr}(0)$. Further, from the multiple image diagram (Young *et. al.* 1980, Blandford and Kochanek 1987), they also showed that multiple images are only possible if $\beta < 1/2$. So, the cross section for NSIS is $\sigma = 0$ for $\beta > 1/2$ and $\sigma = \pi a_{cr}^2$ (with a_{cr} given by equation (23)) if $\beta < 1/2$. In fact, if $\beta < 1/2$, instead of two

(as in SIS), three images are predicted, in agreement with the odd number of images theorem valid for symmetric (non-singular) lenses (Subramanian & Cowling 1986). It can also be shown (Hinshaw and Krauss; see also Hinshaw 1988 for more details) that the angular image separation between the two outer images is given by

$$\theta = \frac{2a_{cr}(0)}{D_{OL}}\left[(1-\beta)^2 - \beta^2\right]^{1/2}. \tag{24}$$

Notice that if $\beta = 0$ the usual result $\theta = 8\pi\frac{D_{LS}}{D_{OS}}\left(\frac{\sigma_{||}}{c}\right)^2$, valid for SIS lenses, is recovered.

In the SIS case, by using equation (21) and assuming conserved comoving number density of lenses ($n_l = n_0(1+z)^3$), equation (11), can be analytically integrated. By using standard distance and statistics we obtain for flat models,

$$\tau(z_S) = \frac{f}{30}\left(d_S(0,z_S)(1+z_S)\right)^3. \tag{25}$$

Here,

$$f = \frac{16\pi^3}{cH_0^3} < n_0\sigma_{||}^4 > \tag{26}$$

measures the effectiveness of the lens in producing multiple images (TOG). An analytic expression for τ in the case of filled beam distance and standard statistics can also be obtained for $k \neq 0$ (see Gott, Park and Lee 1989).

Following FT, we consider the existence of 3 species of galaxies (E, SO and S) and assume a Schechter form for the luminosity function,

$$\Phi(L)dL = \phi^\star(\frac{L}{L^\star})^\alpha \exp(-L/L^\star)\frac{dL}{L^\star}, \tag{27}$$

where $\phi^\star = (1.56 \pm 0.4) \times 10^{-2}h^3Mpc^{-3}$ (Efstathiou, Ellis & Peterson, 1988) is a galaxy number density and $\alpha = -1.1 \pm 0.1$ (see FT). The morphological composition is assumed to be $E : SO : S = 12 : 19 : 69$. We assume, in addition, the relationship, $(\frac{L}{L^\star}) = (\frac{\sigma_{||}}{\sigma_{||}^\star})^\gamma$, between galaxy luminosity and velocity dispersion. Here the exponent γ is, $\gamma = 4$ for E/SO (Faber and Jackson 1976) and $\gamma = 2.6$ for S galaxies (Tully and Fisher 1977). Substitution of (27) in (26) leads to,

$$f = \frac{16\pi^3}{cH_0^3}\phi^\star\sigma_{||}^{\star 4}\Gamma(\alpha + \frac{4}{\gamma} + 1), \tag{28}$$

where $\Gamma(x)$ is the Gamma function and $\sigma_{||}^\star$ is the velocity dispersion corresponding to the characteristic luminosity $L^\star$.

Fukugita and Turner estimated $\sigma_{||}^\star$ to be:

$$\sigma_{||}^\star = \begin{cases} 225^{+12}_{-20} & for\ \text{E}, \\ 206^{+12}_{-20} & for\ \text{SO}, \\ 144^{+8}_{-13} & for\ \text{S}. \end{cases} \tag{29}$$

To take into account dark massive halos, they follow TOG and also adopted a $(3/2)^{1/2}$ correction factor for the velocity dispersions for E/SO galaxies. With the above numbers we find $f_E = 0.018 \pm 0.009$, $f_{SO} = 0.020 \pm 0.011$, and $f_S = 0.007 \pm 0.003$ (total effectiveness parameter, $f = 0.045 \pm 0.023$). More recently Kochanek (1993) argued that the ratio of dark matter dispersion velocity to that of luminous matter should be in the range $0.9 - 1.05$ and suggested that the $(3/2)^{1/2}$ correction factor should not be considered. Without this the factors $f_{E/SO}$ are 2.25 smaller, that is, $f_E = 0.008 \pm 0.004$, $f_{SO} = 0.009 \pm 0.005$ and we get $f = 0.024 \pm 0.012$. We shall consider in the next section these two cases when comparing the predictions of the models with observations.

In Figures 4*a* and 4*b* the normalized optical depth (τ/f), for the four models in the SIS case, is displayed for filled beam distance and standard statistics (Figure 4*a*) and for empty beam distance and Ehlers-Schneider statistics (Figure 4*b*). We also obtained the optical depth for the NSIS case. As discussed before, in this case we should use the appropriate cross section with a_{cr} given by (23). For an analytic expression of the NSIS optical depth in the standard case see Krauss and White (1992). In Figure 5*a* is displayed the NSIS normalized optical depth for filled beam distance (standard statistics). In Figure 5*b* the same quantity is displayed for the empty beam distance (Ehlers-Schneider statistics). A constant value for the core radius, $r_c = 0.5h^{-1}kpc$ and a velocity dispersion $\sigma_{\parallel}^{*} = 144\ km/s$ are assumed for all the models.

The present available data do not allow very good estimates for the core radius of galaxies. In fact, r_c seems to vary a lot even among galaxies with the same morphology. However there is some evidence that most spirals have large core radius ($r_c \gtrsim 0.5$ kpc), although there are also indications that $\sim 10\%$ of them have very small cores (FFKT and references therein). So, in view of the lack of more precise information we assume that 90% of spiral galaxies have a constant core $r_c = 0.5h^{-1}kpc$ and that the remaining 10% are well described by SIS. In fact these assumptions are enough to practically reduce the contribution of S galaxies to the optical depth to only 10% of its SIS value. Actually in case C (cosmological constant), remains another $\sim 1\%$ effect. We can understand this small difference by observing that the quantity $D_{OL}D_{LS}/D_{OS}$ for fixed redshift is higher in case C (see Figure 2). This means that the parameter β tends to be smaller in case C and explains why the effect should be less important in this case. In any case, we confirm the conclusion obtained by Krauss and White, that spiral galaxies have a very small effect on lensing frequencies even if we do not include the $\sqrt{3/2}$ factor in the E/S0 dispersion velocities.

While spirals usually have large core radius, E and SO galaxies are believed to have smaller ones. Most of the analyses of elliptical galaxies are based on slightly different relations between core radius and velocity dispersion (luminosity) that are usually derived by using Lauer's (1985) study of nearby elliptical galaxies. Lauer found that 14 galaxies (from a total number of 42) have resolved cores ($80pc \lesssim r_c \lesssim 400pc$), 23 were unresolved and 5 had marginally resolved cores. By fitting Lauer's data for the resolved cores, Krauss and White obtained a relation between E core

radius and luminosity. By assuming that relation to be valid for all E galaxies they obtained a suppression factor ~ 0.4 for the Einstein-de Sitter model and ~ 0.63 for the cosmological constant dominated universe. Fukugita *et al.* (FFKT) assumed that 1/3 of E galaxies are well described by the relation they obtained from Lauer's study. They also assumed that another 1/3 have core radius given by multiplying that relation by 1/3 and that the remaining 1/3 have $r_c \sim 10pc$. With this model they obtained a suppression factor equal to 0.65. They also claim having changed their assumptions in a reasonable way and always getting numbers between 0.5 and 0.7. We analysed this effect more quantitatively and reached similar results.

We also analysed the core radius effect in the case of empty beam and ES-statistics. We found that the suppression is higher in this case. The reason is that $a_{cr}(0)$ for the empty beam case is smaller and this implies that β is higher, thus increasing the suppression effect. Actually, for spiral galaxies the effect can be very high. For instance, from Figures 4*a* and 4*b* it is clear that τ_{SIS}(z, filled beam)/τ_{SIS}(z, empty beam) is less than one. This means that we should expect a higher frequency of lensed quasars in the open beam case. However by looking at Figures 5*a* and 5*b* we immediately realize that for the special choice of the parameters τ_{NSIS}(z, filled beam)/τ_{NSIS}(z, empty beam) is higher than one and the opposite would be expected. In fact this occurred because we considered in our example a typical spiral galaxy with relatively high core radius and small velocity dispersion. For E/SO galaxies we should expect this effect not to be so conspicuous and, in fact, under reasonable assumptions we obtained a suppression factor that is only $\lesssim 10\%$ higher than that in the filled beam case. In the next section, when comparing model predictions to observations, we will take this small difference into consideration. In order to simplify calculations, we will follow FFKT and assume, for filled beam distance, a constant core effect suppression factor equal to 0.65 for E/SO galaxies. In the case of the empty beam we will consider a suppression factor equal to 0.60.

By using the filled beam distance, standard statistics and the SIS profile it can be shown (see FT and FFKT) that the normalized image angular separation distribution for a source at z_S is given by

$$\frac{dP}{d\theta}(z_S,\theta) = \frac{1}{\tau(z_S)}\int_0^{z_S}\frac{d^2\tau}{dz_L d\theta}dz_L$$

$$= \frac{f}{\tau(z_S)}\int_0^{z_S}(1+z_L)^3\left(\frac{D_{OL}D_{ls}}{cH_0{}^{-1}D_{OS}}\right)^2\left(-\frac{1}{cH_0^{-1}}\frac{cdt}{dz_L}\right)\times$$

$$\frac{\gamma/2}{\Gamma(\alpha+1+\frac{4}{\gamma})}\left(\frac{D_{OS}}{D_{LS}}\frac{\theta}{8\pi\left(\frac{\sigma_{\parallel}^*}{c}\right)^2}\right)^{\frac{\gamma}{2}(\alpha+2)}\exp\left[-\left(\frac{D_{OS}}{D_{LS}}\frac{\theta}{8\pi\left(\frac{\sigma_{\parallel}^*}{c}\right)^2}\right)^{\frac{\gamma}{2}}\right]\frac{1}{\theta}dz_L. \qquad (30)$$

In Figure 6*a* the predicted image separation distribution for a source at redshift $z_S = 2.2$ (the quasar average redshift in the HST snapshot survey) is shown in two

cases for E/SO galaxies. We took $\alpha = -1.1$, and to simplify the computation we considered the same velocity for E and SO galaxies, that is we chose an average velocity, $\sigma_{||}^{\star} = 213 \times \sqrt{\frac{3}{2}}\ km/s$ in case (i) and $\sigma_{||}^{\star} = 213\ km/s$ in case (ii). The same quantity for both cases is also displayed in Figure 6*b* for the empty beam distance and Ehlers-Schneider statistics. In this case we took into account equation (15) in the definition of the differential optical depth. Figure 6a shows that for flat models and filled beam distance the image separation distribution is independent of m and Ω_{m0}. In fact, as remarked by FFKT, it is also independent of z_S. For empty beam distance the degeneracy of flat models is broken and we can observe a shift of the distribution to smaller values of angular separation. It is also clear that in both cases increasing the velocity dispersion increases the probability of larger image separation.

4 Comparison with observations

In this section we shall compare the predicted number of multiple images (and their angular image separation) for the models presented in section 2 with the observational results of the Hubble Space Telescope Snapshot Survey (Maoz *et al.* 1993). In the last report of the survey, Maoz *et al.* announced the existence of six lens candidates from a sample of 502 quasars. In fact, two of the lensed candidates have unexpectedly large image separation. There is evidence that one of them was produced not by a single galaxy but by a more complex system, and it is not clear that the other one is really a multiple image of one single object (Maoz and Rix and references therein) . Following the current interpretation, we shall not include these two cases in our analysis. The four remaining candidates have the following redshift and image separation (z,θ): (3.8, 0.47"), (2.55, 1.22"), (1.72, 2.0") and (2.72, 2.2").

The expected number of lensed quasars in the survey (N_E), for each model, is obtained by computing the quantity

$$N_E = \sum_{i=1}^{N_Q} \tau(z_i) \tag{31}$$

where the sum is over the N_Q quasars redshifts of the survey. In calculating the expected number of multiple images, besides the core radius effect that we discussed in the last section, we also took into account two other corrections to τ, namely, the angular selection effect ($\times 0.95$ for E and SO) and magnification bias ($\times 9.1$) (see Fukugita and Peebles).

In Table 1 we display, for each model, the predicted number of lensed quasars for the HST snapshot survey. The numbers were obtained for filled beam and standard statistics as well as for empty beam and Ehlers-Schneider statistics. We show results for the cases in which we have and have not included the $(3/2)^{1/2}$ factor in velocity dispersion. By assuming Poisson statistics we also display, for all cases, the probability of detecting the observed number (four) of lensed quasars. Notice that in case C the

final results depend considerably on the assumptions performed. For instance, if we take into account the $(3/2)^{1/2}$ factor, the predicted number of lensed quasars is too high in model C. However if we do not consider the correction the model cannot be ruled out, at least based only on the total number of images. From Table 1 we also see that model D is the least sensitive to the assumptions and seems to be in good agreement with observations. It is also clear that the lensing rate is a factor ~ 2 smaller in model B than in model C and this corroborates the idea that usually decay Λ models have a lower lensing rate than the constant Λ ones. We should remark that this is not always true and some decaying Λ models can, in fact, predict very large lensing rates.

Recently Kochanek (1993) pointed out that analyses based only on Poisson statistics give no weight to the different ways that a fixed number of multiple images is produced. He then suggested a maximum likelihood method that takes this into account. His technique is based on the following likelihood function,

$$L = \prod_{i=1}^{N_U}(1-p_i)\prod_{j=1}^{N_L} p_j \prod_{k=1}^{N_L} p_{ck}. \tag{32}$$

Here N_U is the number of unlensed quasars, N_L is the number of lensed ones, $p_i \ll 1$ is the probability that quasar i is lensed and p_{ck} is the configuration probability, that we shall consider as the probability that quasar k is lensed with the observed image separation.

We applied Kochanek technique to the flat models. By expressing L as a function of the parameters m and Ω_{m0} we obtained the maximum of the likelihood function (L_{max}) and formed the ratio $l = L/L_{max}$. It can be shown that with two parameters, the distribution of $-2\ln l$ tends to a χ^2 distribution with two degrees of freedom (Kendall & Stuart 1977, Eadie *et al.* 1971, Kochanek 1993).

Contours of constant likelihood are plotted in Figure 7. Regions with larger likelihood are represented by lighter shades. The maximum of the likelihood is indicated by a cross (+). We should remark that the figure is very broad and is displayed to give a qualitative view of the likelihoods. For the figure we considered the value of the velocity dispersion equal to 213 km/s. We observed that the results did not change appreciably when we increased the velocity dispersion to $\sigma_{\|}^{\star} = 261$ km/s. Some qualitative aspects can be inferred from the figure. For instance, if m is low ($m \lesssim 0.5$) regions with a lower value of Λ, let say, those with $\Omega_{m0} \gtrsim 0.4$, have higher likelihood. However if $m \gtrsim 2$ that constraint does not exist and models with low Ω_{m0} are in fact more likely. We observe that in the two-dimensional space of the parameters of Figure 7, the Einstein-de Sitter models is represented by two points. The first one is $m = 0$ and $\Omega_{m0} = 1$, while the second one is obtained by taking the limit $m \to 3$ and $\Omega_{m0} \to 0$. Figure 8 gives more quantitative information. We plot in it the 50%, 68%(1σ) and 95.4%(2σ) confidence levels for the likelihood ratio for the two parameters.

It is important to emphasize that our main goal in this paper was not to obtain constraints on possible values of a constant Λ. Our target in this work was rather to show that if Λ is not constant, the lensing constraints on Ω_Λ are much weaker. In fact we found that regions with higher values of m and lower Ω_{m0} present larger likelihood. However, if we want to make some comparison with previous results, as for instance those of Kochanek (1993), we should fix the parameter m to the value $m = 0$ (cosmological constant). In this case the likelihood peaks at $\Omega_{m0} = 0.62$ but now we have that $-2\ln l$ is distributed like a χ^2 distribution with one degree of freedom. In this case the constraints on Λ are stronger and, for instance, we get $\Omega_\Lambda \lesssim 0.8$ at 90% confidence level. We remark that we have not obtained one of Kochanek's constraints, $\Omega_\Lambda \lesssim 0.45$, for the following reasons. First, as we discussed, we were only considering lensing by galaxies, so we have not included in our analysis the lens 0957+561. Second, we have used the SIS profile but we took into account a core radius suppression effect. Third, in our likelihood analysis we neglected the contribution of spiral galaxies.

5 Discussion and conclusion

As is well known, a sufficiently long period of inflation in the early universe gives a natural solution to the isotropy, flatness, and monopole problems. A nearly invariant primordial spectrum is also generated in most of the inflationary models of the universe, a feature that seems to be in good agreement with observations. Inflationary models usually predict $\Omega_{total} = 1$. Nevertheless, observations on the scales $10 - 30$ Mpc, based on dynamical methods, indicate $\Omega_{m0} = 0.2 \pm 0.1$. Further, in flat models with $\Omega_{m0} = 1$ only if $h \leq 0.59$ is it possible to get theoretical ages in agreement with the lowest age estimates ($t_0 = 11Gyr$) for globular clusters. However, most of the recent observations indicate higher values for the Hubble parameter. Besides, the standard CDM model ($\Omega_{m0} = 1$ and $h = 0.5$) when normalized to COBE predicts more power on small scales than is observed, and some of its variants such as $HCDM$ seem to work well only if $h \sim 0.5$ (Primack 1995). By assuming a non-zero cosmological constant all these problems can be solved at once while keeping the attractiveness of inflation.

Cosmologists in general show an enormous resistance in accepting the idea of a non-zero cosmological constant for several reasons. First, because it is another parameter in the theory and from an aesthetic point of view this makes Λ-models less compelling. The second reason is that in order to dominate the dynamics of the universe only recently, this parameter should have a very small value ($\Lambda \lesssim 10^{-56} cm^{-2}$) that is in fact 50 to 120 orders of magnitude below the estimate given by quantum field theory. If we assume a decaying cosmological term, this second problem is alleviated but we have to pay the price of introducing another parameter. In this paper we have also discussed a weakness on the observational side of constant-Λ models. It is the prediction of too high frequency of lensed quasars by models with

a large cosmological constant. Ratra and Quillen showed that the predicted lensing rate is considerably reduced in certain models in which a scalar field plays the role of an effective decaying Λ-term. In this paper we reached the same conclusion for models in which the cosmological term decreases with time as $\Lambda \propto a^{-m}$. We went one step further and also showed that for these models, lower values of Ω_{m0} and larger m have higher likelihood. Finally, we should mention that by increasing the value of the parameter m, and maintaining constant the value of Ω_{m0}, the theoretical age predicted by the models we have considered decreases. So, it would be interesting to extend the likelihood analysis by also taking into account the age constraints. Further investigation in this direction is being carried out.

Acknowledgements

We would like to thank Josh Frieman for critically reading the manuscript and for several useful suggestions. We also would like to thank Luca Amendola, and Scott Dodelson for helpful discussions and Edgar Oliveira for calling our attention to a useful reference on statistics. This work was supported in part by the Brazilian agency CNPq and by the DOE and NASA at Fermilab through grant NAG5-2788.

References

Abdel-Rahman, A-M. M.: 1992, *Phys.Rev.* **D45**, 3497.
Blandford, R.D., Kochanek, C.S.: 1987, *'Dark matter in the Universe', World Scientific, Singapore*, p. 133, "Gravitational lenses", edited by J. Bahcall, T. Piran and S. Weinberg
Bourassa, R. R., Kantowski, R.: 1975, *Astrophys. J.* **195**, 13.
Carrol, S. M., Press, W. H., Turner, E. L.: 1992, *Annual Review of Astron. Astrophys.* **30**, 499.
Carvalho, J. C., Lima, J. A. S., Waga, I.: 1992, *Phys. Rev.* **D46**, 2404.
Chaboyer, B.: 1995, "Absolute ages of globular clusters and the age of the Universe", submitted to ApJ *Letters*, astro-ph 9412015.
Chen. W., Wu, Y. S.: 1990, *Phys. Rev* **D41**, 695.
Dyer, C.C., Roeder, R.C.: 1972, *Astrophys. J.* **174**, L115.
Dyer, C. C., Roeder, R. C.: 1973, *Astrophys. J.* **180**, L31.
Eadie, W. T., *et al.*: 1971, "*Statistical methods in experimental physics*", North-Holland Publishing Company.
Efstathiou, G., Sutherland, W. J. & Maddox, S. J.: 1990, *Nature* **348**, 705.
Ehlers J. and Schneider P.:1986, *Astron. Astrophys.* **168**, 57.
Faber, S., Jackson, R.: 1976, *Astrophys. J.* **204**, 668.
Feldman, H. A., Evrard, A. E.: 1993, *Int. J. Mod. Phys.* **D2**, 113.
Freedman, W. L., *et al.*: 1994, *Nature* **371**, 757.
Freese, K., Adams, F. C., Frieman, J. A., Mottola, E.: 1987, *Nucl. Phys.* **B287**, 797.
Fry, J. N.: 1985, *Phys. Lett.* **B158**, 211.
Fukugita M., Futamase T., Kasai M.: 1990, *Monthly Notices Roy. Astron. Soc.* **246**,

24p.
Fukugita M., Futamase T., Kasai M., E. L. Turner: 1992, *Astrophys. J.* **393**, 3.
Fukugita, M., Peebles, P.J.E.: 1993, *Astrophys. J., submitted*, "Visibility of gravitational lenses and the cosmological constant problem"
Hinshaw, G.: 1988, "*Topics in gravitational theory*", PhD thesis, Harvard University.
Hinshaw, G., Krauss, L.M.: 1987, *Astrophys. J.* **320**, 468.
Kendall, M., Stuart, A.: 1977, "*The advanced theory of statistics*", Volume 2, 4^{th} edition, Charles Griffen, London.
Kochanek, C.S.: 1993, *Astrophys. J.* **419**, 12.
Kofman, L. A., Gnedin, N. Y., Bahcall, N. A.: 1993, *Astrophys. J.* **413**, 1.
Krauss, L., White, M.: 1992, *Astrophys. J.* **394** , 385.
Lahav, O., Lilje, P. B., Primack, J. R.& Rees, M. J.: 1991, *Monthly Notices Roy. Astron. Soc.* **251**, 128.
Lodge, O. J.: 1919, *Nature* **104**, 354.
Mao, S.: 1991, *Astrophys. J.* **380**, 9.
Mao, S., Kochanek, C.S.: 1994, *Monthly Notices Roy. Astron. Soc., submitted*, "Limits on galaxy evolution"
Maoz, D., *et al.* : 1993, *Astrophys. J.* **409**, 28.
Maoz, D., Rix, H. W.: 1993, *Astrophys. J.* **416**, 425.
Martel, H.: 1995, "Nonlinear structure formation in flat cosmological models", to appear in *Astrophys. J.*, University of Texas McDonald Observatory preprint No. 305.
Ozer, M., Taha, M. O.: 1987a, *Phys. Lett.* **B171**, 363.
Ozer, M., Taha, M. O.: 1987b, *Nucl. Phys.* **B287**, 776.
Peebles P. J. E.: 1984, *Astrophys. J.* **284**, 439.
Peebles P. J. E.: 1993, "*Principles of physical cosmology*", Princeton University Press.
Peebles,P. J. E., Ratra, B.: 1988, *Astrophys. J.* **325** , L17.
Pierce, M. J., *et al.*: 1994, *Nature* **371**, 385.
Press, W.H., Gunn, J.E.: 1973, *Astrophys. J.* **185**, 397.
Primack, J. R.: 1995, *Status of cosmological parameters: Can* $\Omega = 1$*?*, to appear in the "Proceedings of Particle and Astrophysics in the Next Millenium", eds. E. W. Kolb and R. Peccei, World Scientific.
Ratra, B., Peebles, P. J.E.: 1988. *Phys. Rev.* **D37**, 3407.
Ratra B., Quillen A.: 1992, *Monthly Notices Roy. Astron. Soc.* **259**, 738.
Refsdal S.: 1964, *Monthly Notices Roy. Astron. Soc.* **128**, 307.
Rix, H.-W., Maoz, D., Turner, E.L., Fukugita,M.: 1994, *Astrophys. J., submitted*, "Galaxy mergers and gravitational lens statistics"
Sahni, V., Feldman, H. A., Stebbins, A.: 1992, *Astrophys. J.*, **385**, 1.
Schneider P., Ehlers J., Falco E. E.: 1992, "*Gravitational Lenses*", Springer-Verlag.
Silveira V., Waga I.: 1994, *Phys. Rev* **D50**, 4890.
Subramanian, K., Cowling, S.A.: 1986, *Monthly Notices Roy. Astron. Soc.* **219**, 333.

Tully, R. B., Fisher, J.: 1977, *Astron. Astrophys.*, **54**, 661.
Turner, E.L.: 1990, *Astrophys. J.* **365**, L43.
Turner E. L., Ostriker J. P. , Gott III J. R.: 1984, *Astrophys. J.* **284**, 1, (1984).
Turner M. S., Steigman G. & Krauss L. M.: 1984, *Phys. Rev. Lett.* **52**, 2090.
Vilenkin A.: 1984, *Phys. Rev. Lett.* **53**, 1016, (1984).
Young, P., Gunn, J.E., Kristian, J., Oke, J.B., Westphal, J.A.: 1980, *Astrophys. J.* **241**, 507

Table 1: **Predicted number of lensed quasars for the HSTSS and model probabilities**

	model A $k=0$ $\Omega_{m0}=1$	model B $k=0, m=2$ $\Omega_{m0}=0.2$	model C $k=0, m=0$ $\Omega_{m0}=0.2$	model D $k=-1$ $\Omega_{m0}=0.2$
filled beam (with $\sqrt{3/2}$)	2.6	4.7	10.7	4.1
probability	18%	17%	0.3%	19%
empty beam (with $\sqrt{3/2}$)	4.2	7.1	14	4.6
probability	19%	6%	10^{-2}%	18%
filled beam (without $\sqrt{3/2}$)	1.2	2.2	5.0	1.9
probability	9%	16%	16%	14%
empty beam (without $\sqrt{3/2}$)	1.9	3.3	6.8	2.1
probability	14%	20%	7%	15%

Figure Captions

Figure 1: Dyer-Roeder distance as a function of the redshift; (a) filled beam and (b) empty beam.

Figure 2: The combination $D_{OL}D_{LS}/(D_{OS}cH_0^{-1})$ as a function of z_L ; (a) filled beam distance and (b) empty beam distance.

Figure 3: Lensing geometry.

Figure 4: The normalized optical depth (τ/f) as a function of the redshift for the SIS case; (a) is for filled beam distance and standard statistics and (b) for empty beam distance and Ehlers-Schneider statistics.

Figure 5: The normalized optical depth (τ/f) as a function of the redshift for the NSIS case; (a) is for filled beam distance and standard statistics and (b) for empty beam distance and Ehlers-Schneider statistics. For all the plots we assumed $r_c = 0.5h^{-1}kpc$ and $\sigma_{||}^{*} = 144\ km/s$.

Figure 6: Distribution of the angular image separation for a source at $z_S = 2.2$ in SIS case. We took $\alpha = -1.1$, $\gamma = 4$ and considered in case (i) $\sigma_{||}^{*} = 261\ km/s$ and in (ii) $\sigma_{||}^{*} = 213\ km/s$; (a) filled beam and standard statistics and (b) empty beam and Ehlers-Schneider statistics.

Figure 7: Contours of constant likelihood for flat models are plotted in the Ω_{m0} and m parameter space. Regions with larger likelihood are represented by lighter shades. The peak of the likelihood is indicated by the cross.

Figure 8: Likelihood contours at 50%, 68%(1σ) and 95.4%(2σ) confidence levels for the two dimensional likelihood distribution l.

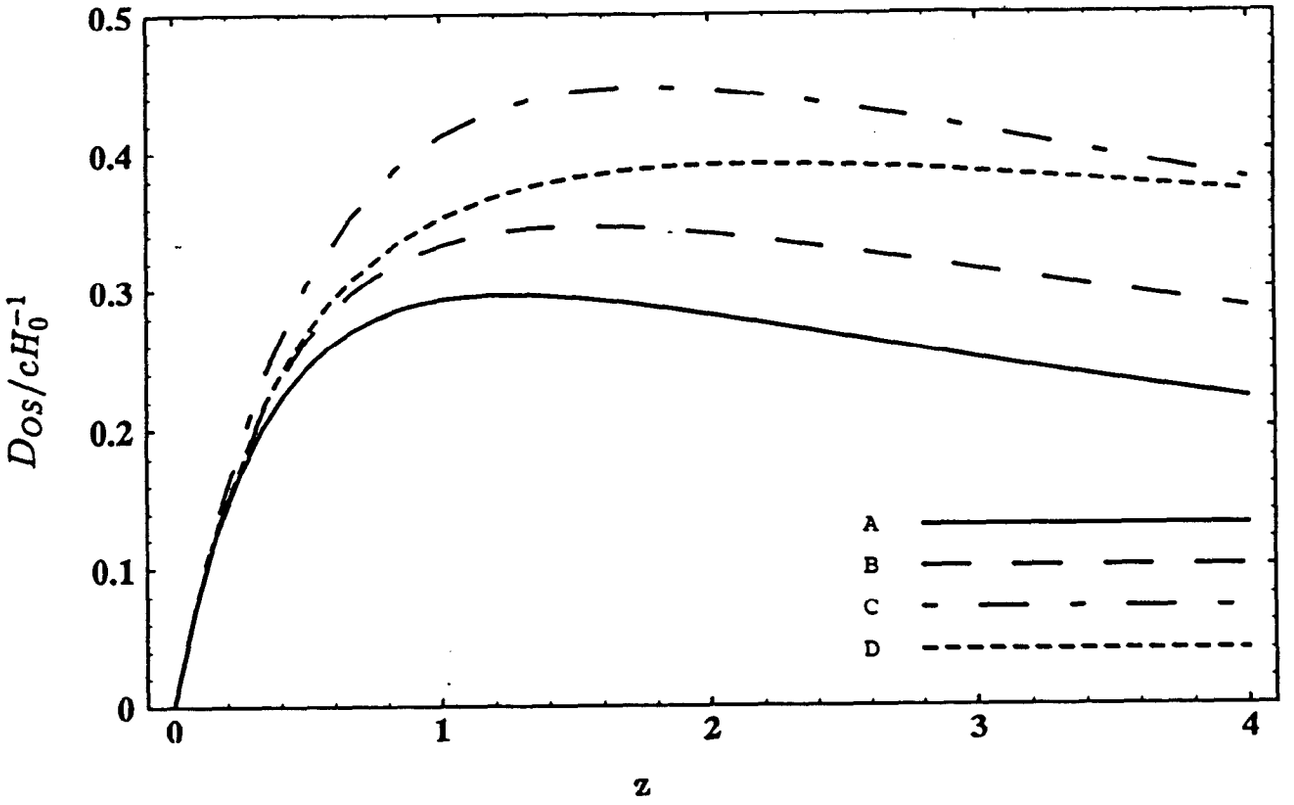

Figure 1a

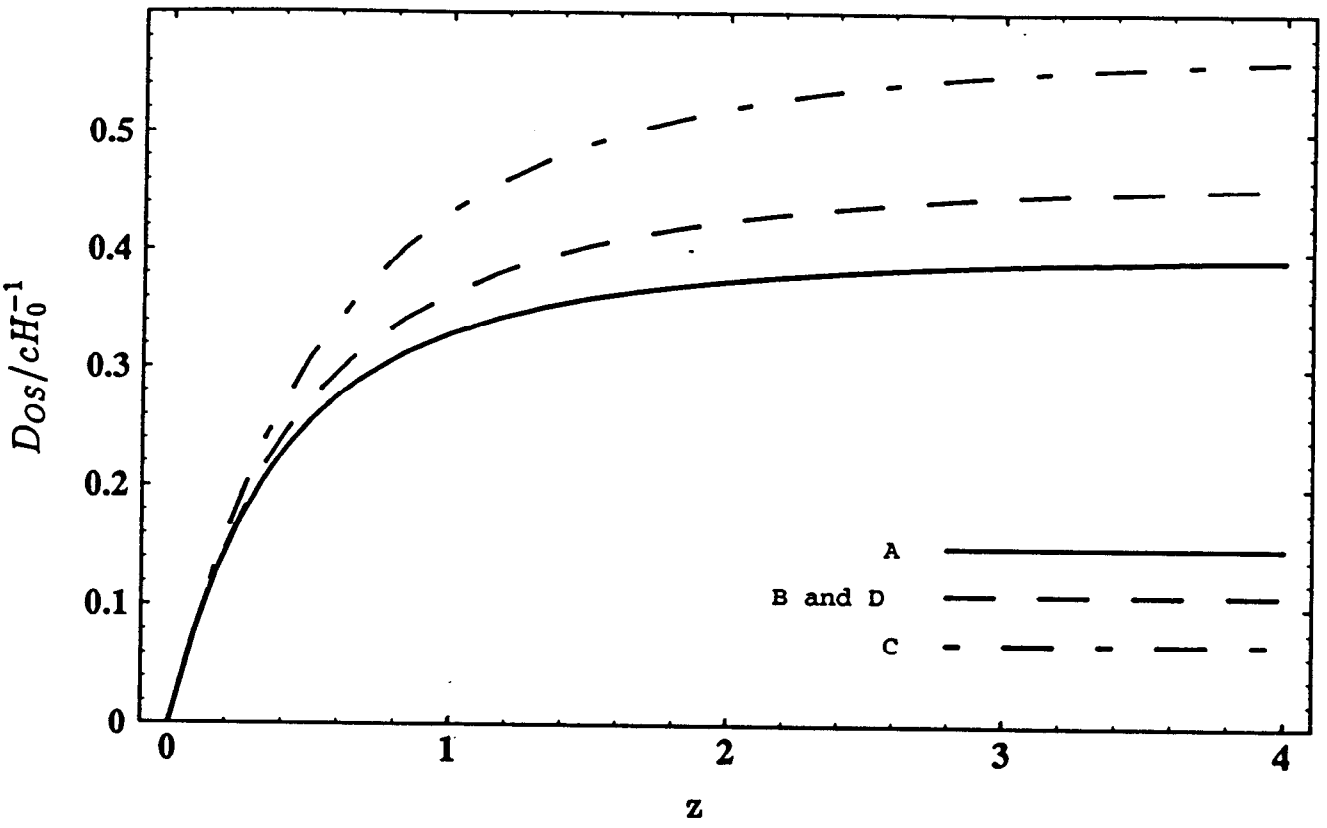

Figure 1b

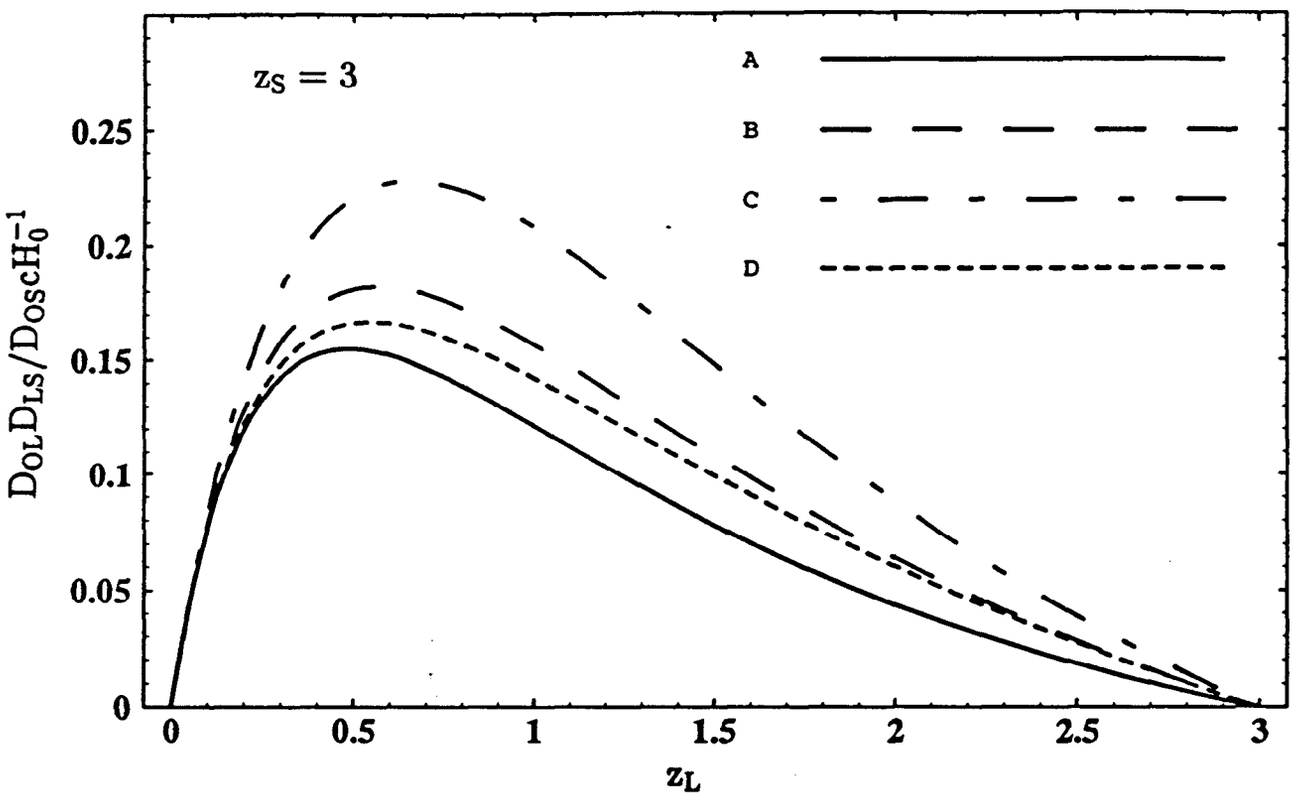

Figure 2a

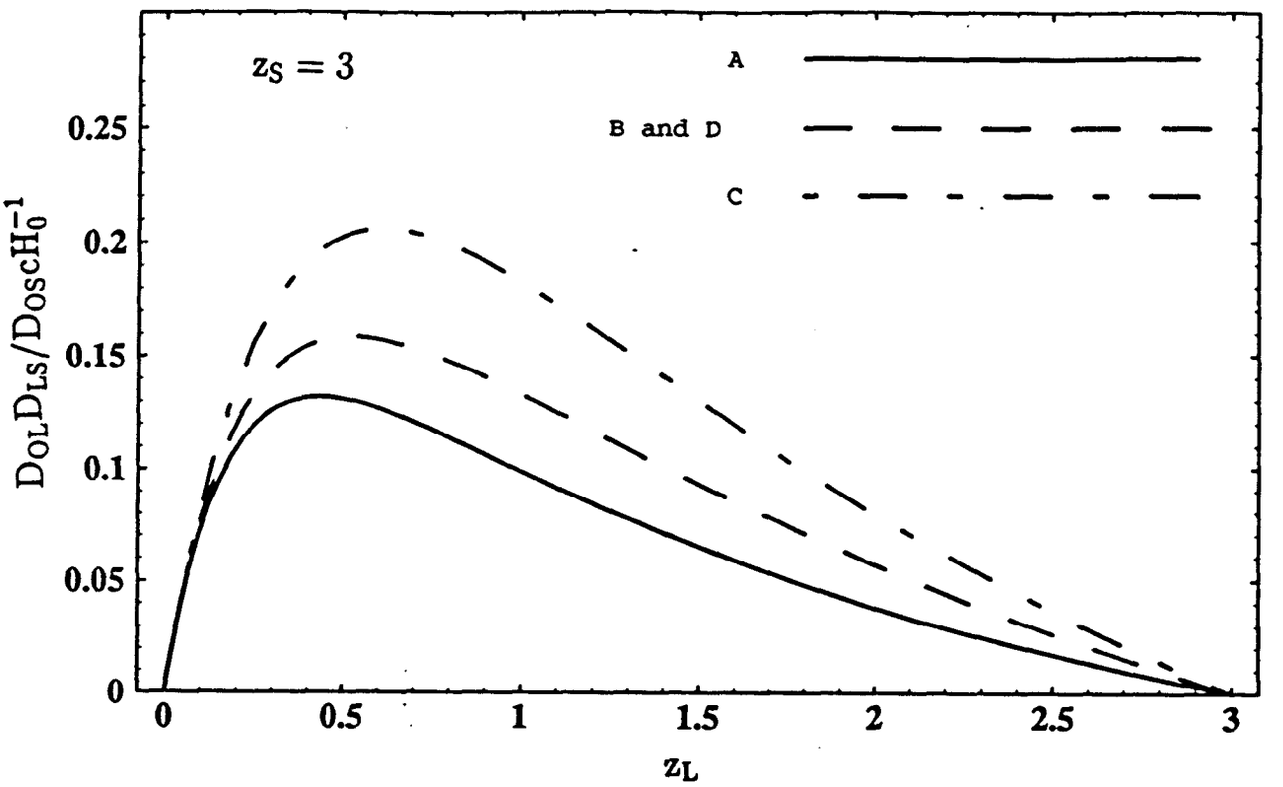

Figure 2b

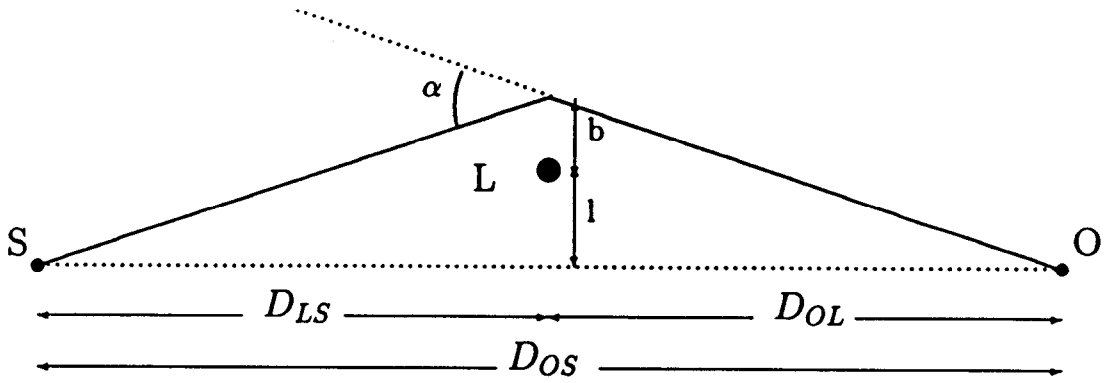

Figure 3

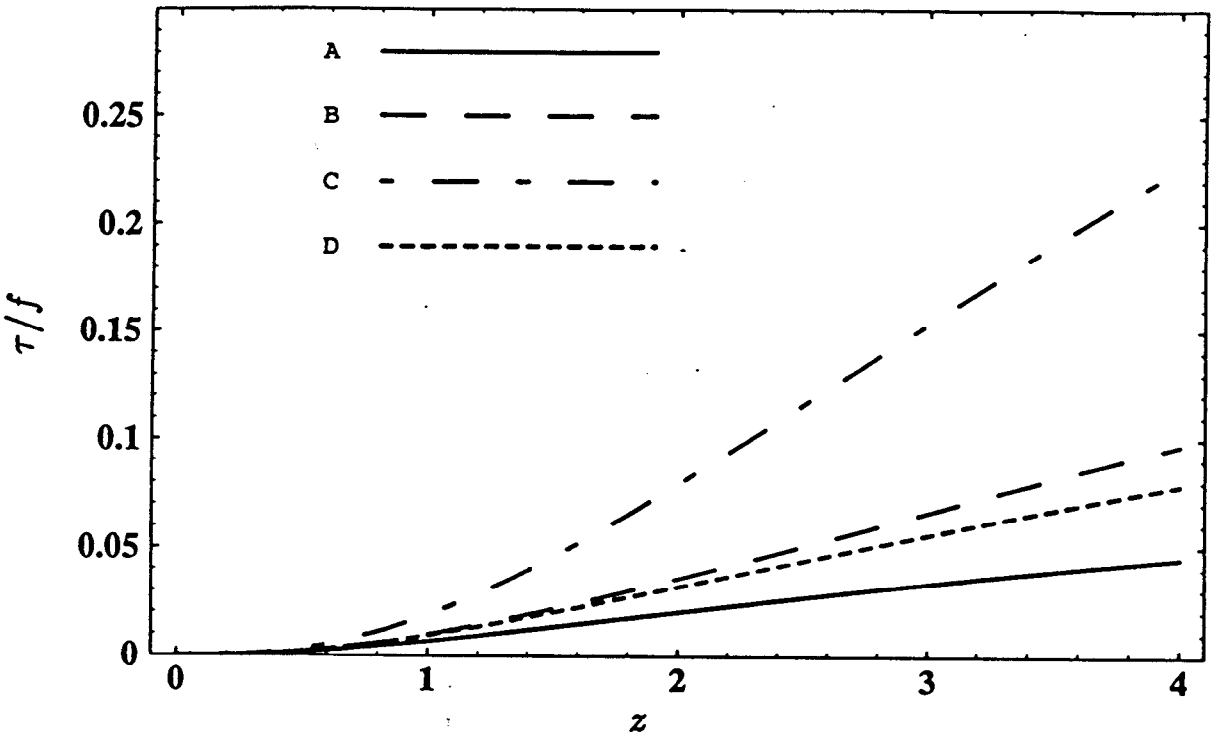

Figure 4a

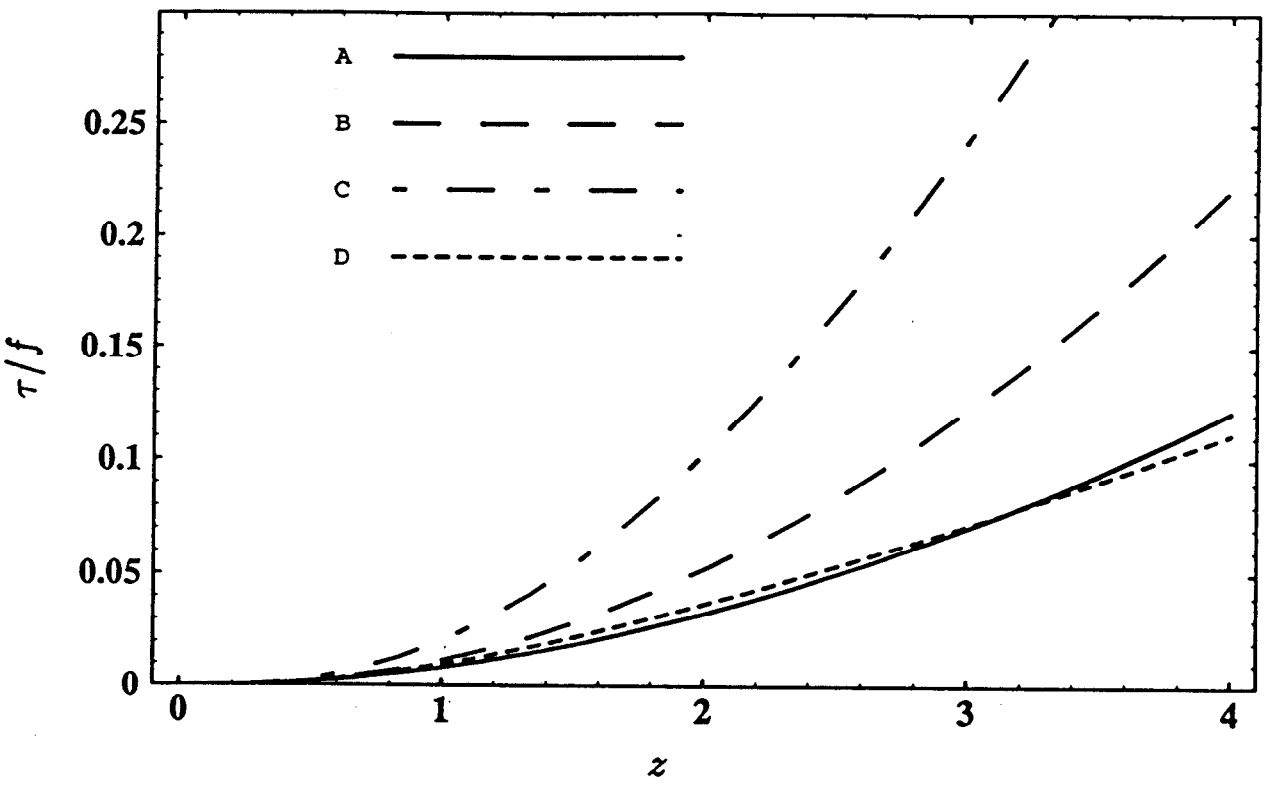

Figure 4b

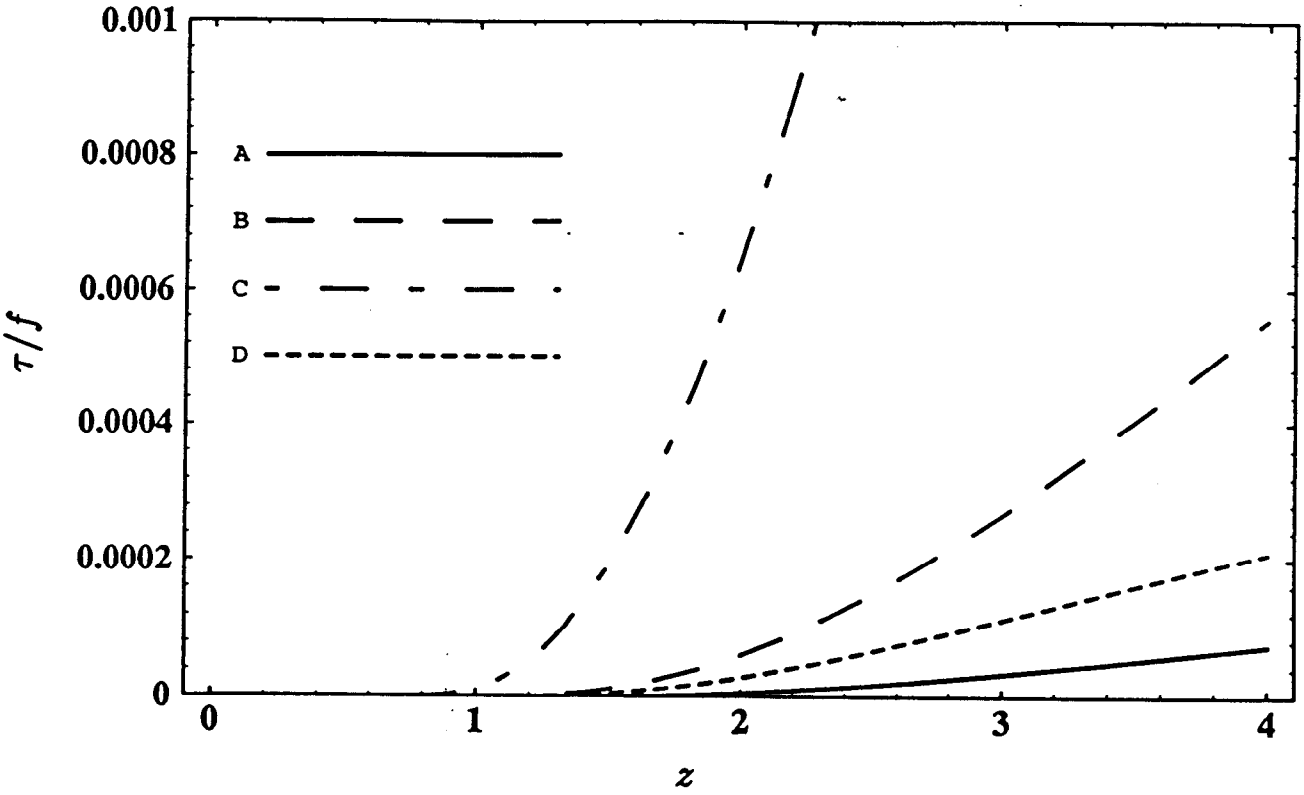

Figure 5a

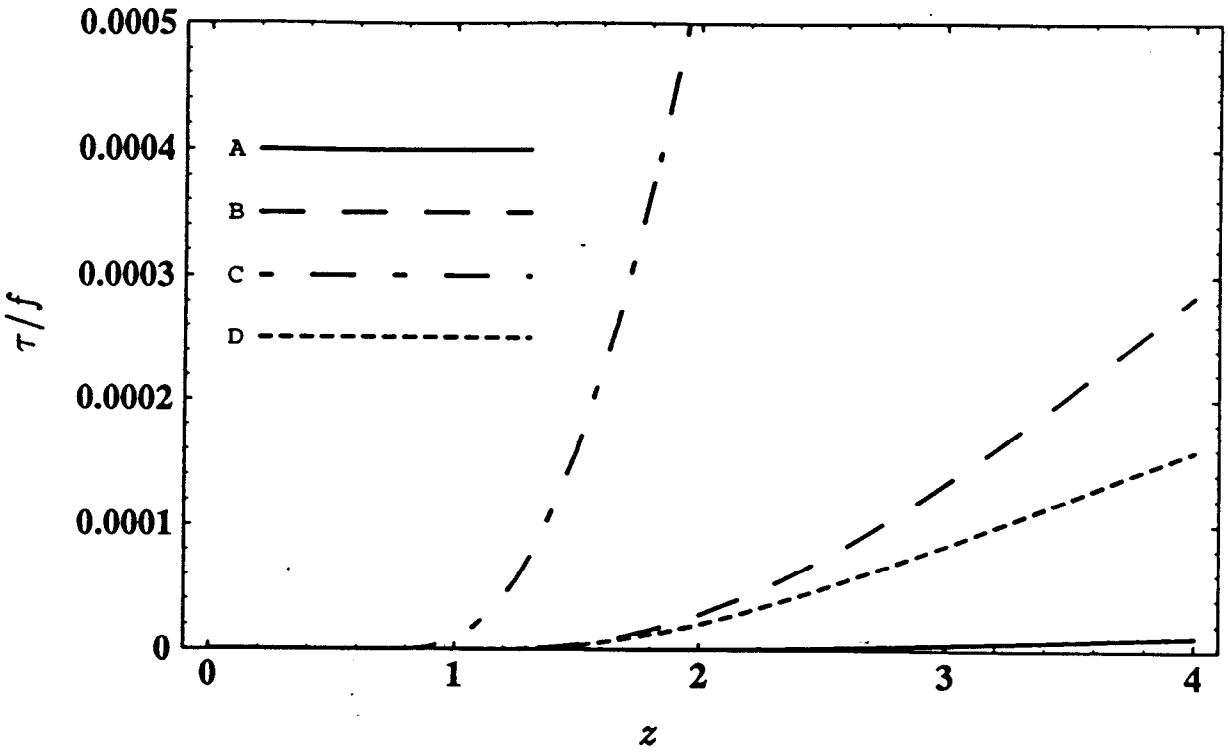

Figure 5b

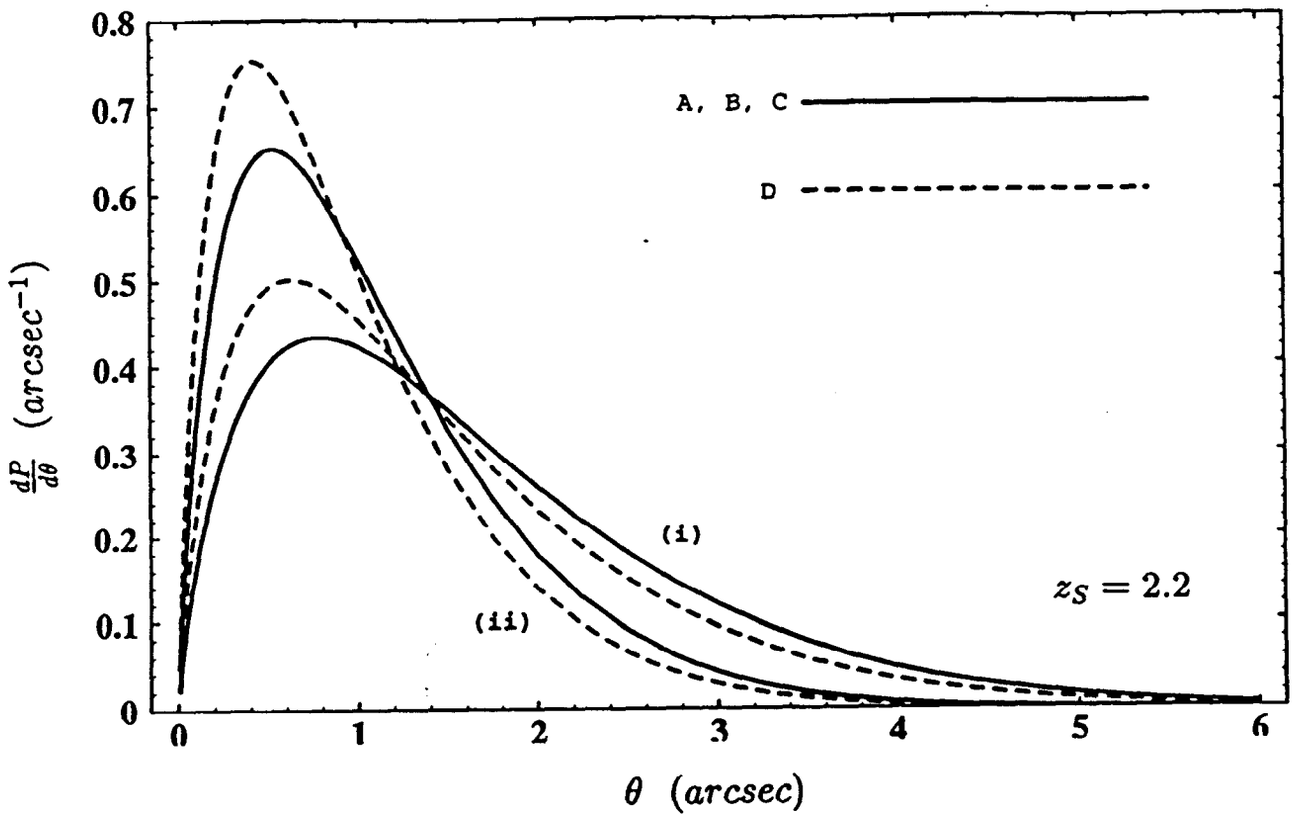
0.8
0.7
0.6
0.5
0.4
0.3
0.2
0.1
0
0
1
2
3
4
5
6
A, B, C
D
(i)
(ii)
$z_S = 2.2$
$\frac{dP}{d\theta}$ $(arcsec^{-1})$
θ $(arcsec)$

Figure 6a

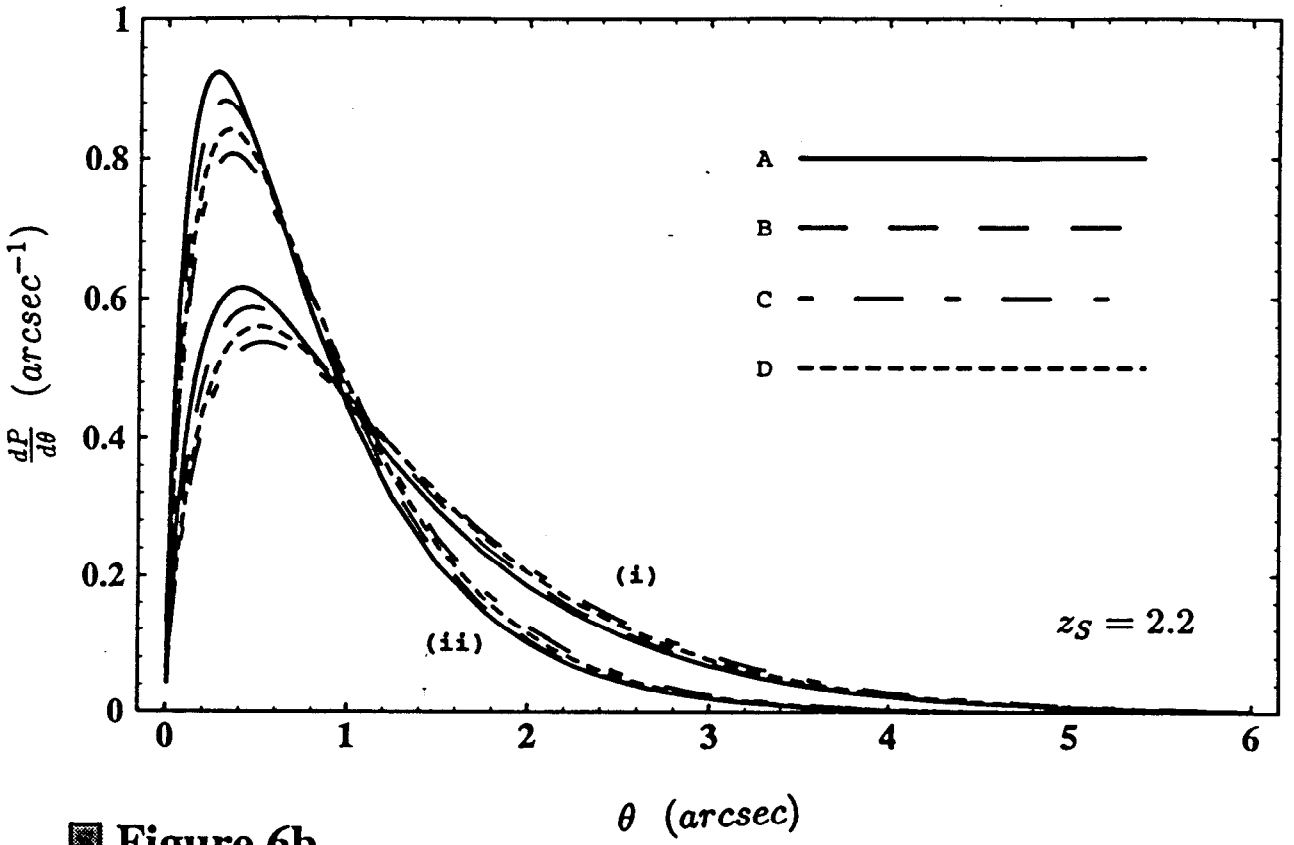
1
0.8
0.6
0.4
0.2
0
0
1
2
3
4
5
6
$\frac{dP}{d\theta}$ $(arcsec^{-1})$
θ $(arcsec)$
A
B
C
D
(i)
(ii)
$z_S = 2.2$

Figure 6b

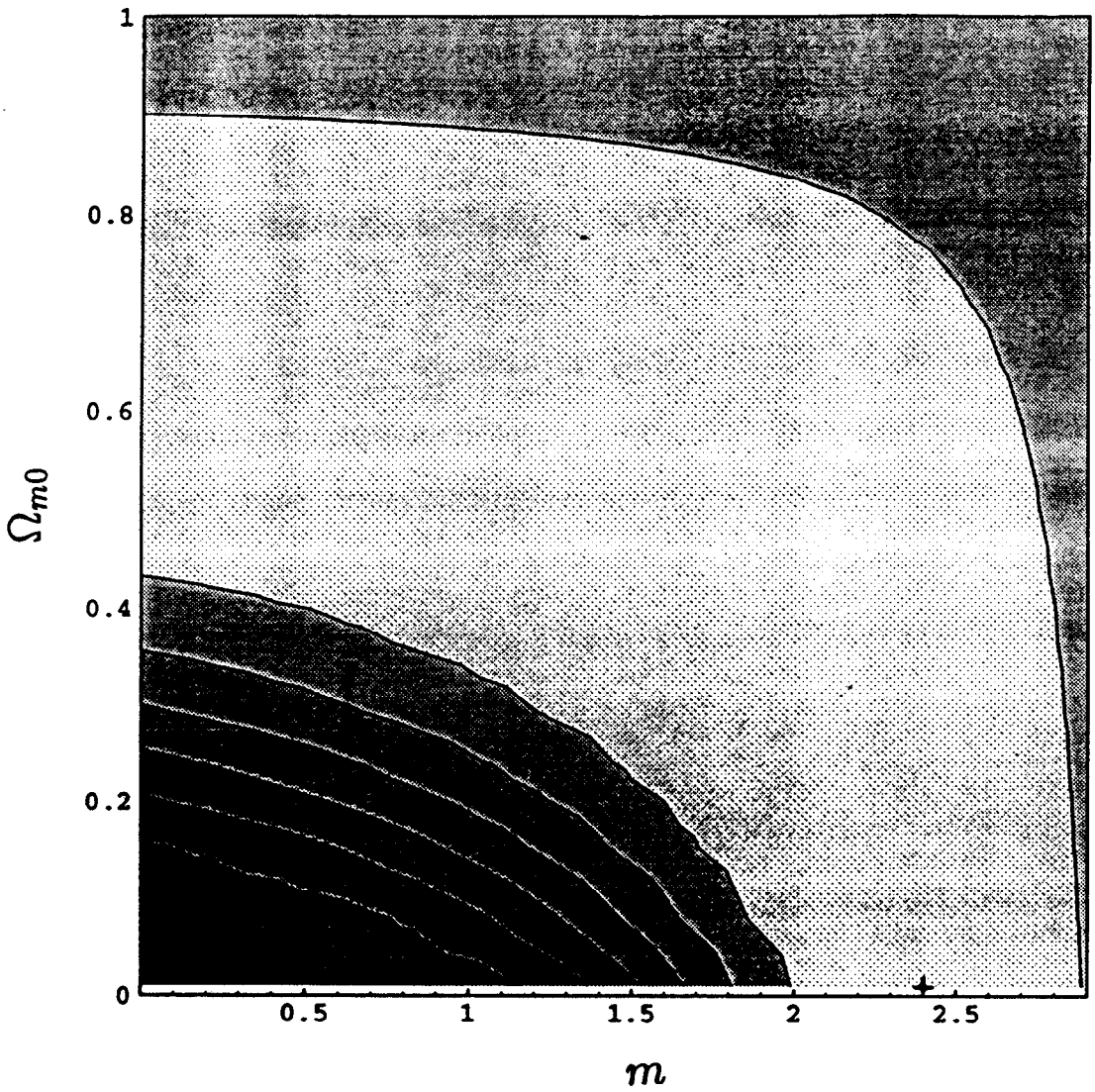

Figure 7

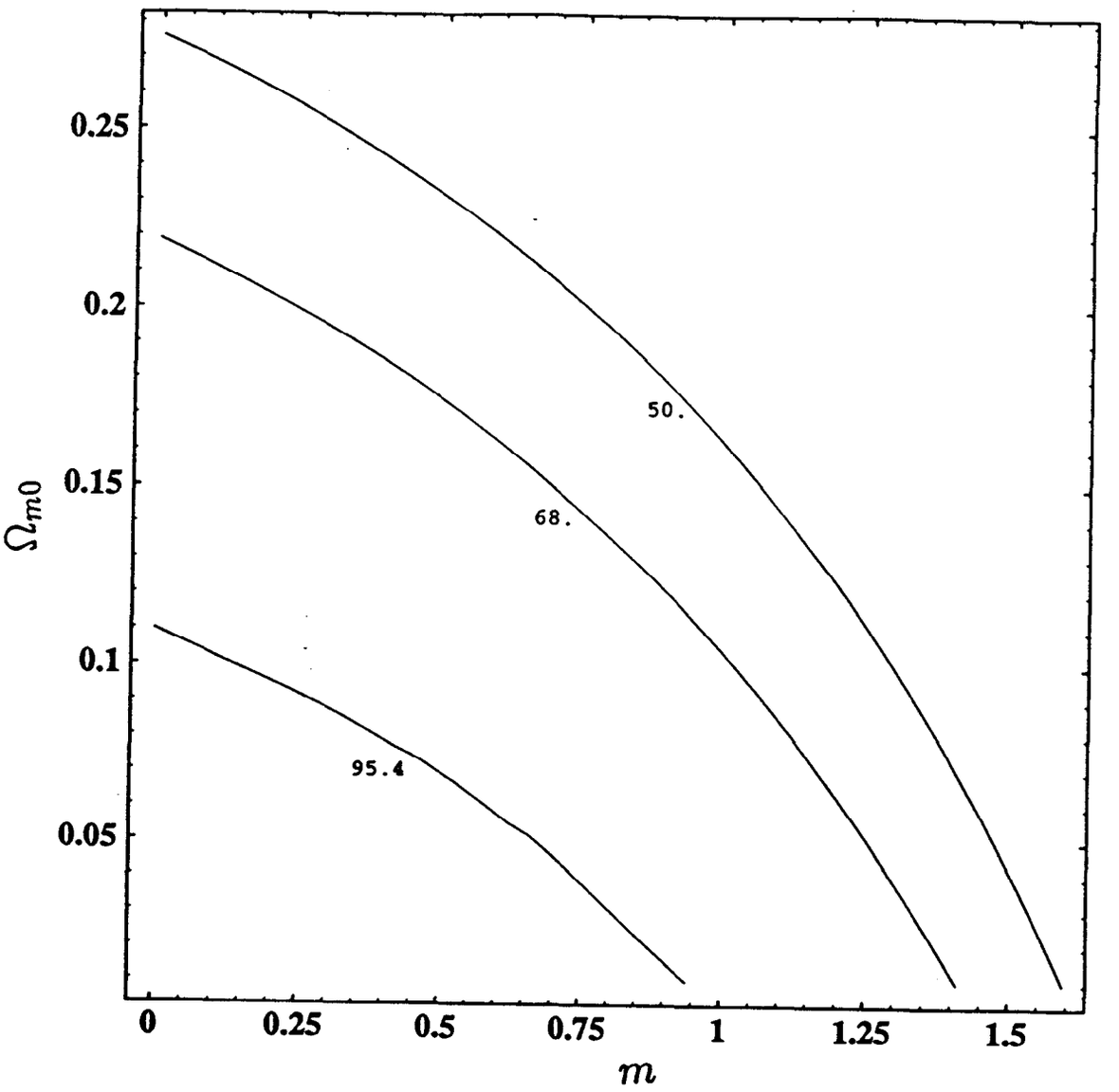

Figure 8